Seismic Effect on Shear Band Development in Soil Slope

Vijay Kumar (vijayk.phd20.ce@nitp.ac.in)
National Institute of Technology
Sunita Kumari
National Institute of Technology

Research Article

Keywords: Seismic load, Soil Slope, Shear Band, Strain Localization, Plain Strain

Posted Date: April 22nd, 2022

DOI: https://doi.org/10.21203/rs.3.rs-1546728/v1

SEISMIC EFFECT ON SHEAR BAND DEVELOPMENT IN SOIL SLOPE

Vijay Kumar[1], Sunita Kumari[2]

1. Research Scholar, Department of Civil Engineering, National Institute of Technology, Patna, India. Email: vijayk.phd20.ce@nitp.ac.in
2. Associate Professor, Department of Civil Engineering, National Institute of Technology, Patna, India

Abstract

The present study discusses the impact of seismic load on shear band development in soil slope is using finite element modeling considering plain strain condition. Large inelastic deformations are frequently accompanied with the formation of intense bands of localized shearing which results large strain plastic response. Shear band formation is considered as significant factor to understand failures in soil slope. The strain analysis has been performed considering maximum shear strain to investigate the shear deformation behavior of the slope of soil deposit. To simulate the strain localization, softening behavior and development of shear band, a Modified Cam-Clay (MCC) material model was implemented. It is found that none of the slopes are stable under seismic action, but the instability of different slopes with inclination varies. The slope with an inclination of 1:2.25 is relatively stable. The slope with an inclination of 1:2 has local failure, but not destroyed as a whole. The slope with an inclination of 1:1.75 has a complete formation of shear band along the slip surface. The slope is destroyed as a whole. Hence, both tension and strain localization causes deformation in slope. Displacement and acceleration response was found maximum at the crest of slope.

Keywords: Seismic load, Soil Slope, Shear Band, Strain Localization, Plain Strain.

Introduction

The strain softening behavior of geotechnical material generally leads to progressive failure (Skempton, 1964; 1985; Mesri and Shahien, 2003; Conte et al., 2010; Locat *et al.*, 2011). This type of failure occurs either in tension or localization of strain in soil mass. Further, it was studied that most of the geotechnical engineering problems occur either by the formation of narrow shear band or localization of large shear strain. The localized behavior and formation of shear band have been confirmed by a number of field observations and model tests (Burland *et*

al. 1977; Torabi, 2007; Wang and Zhang 2014; Zhang *et al*. 2015) as well as theoretical studies (Vardoulakis, 1996 and Sadrekarimi, 2009). Based on theoretical and laboratory considerations, it is found that shear band formation is most prominent in softening material. Failure of a plane strain specimen always occurred along a well-defined shear zone. This phenomenon of shear zone and progressive failure are observed and analyzed with the application of various loads, such as seismic load (Cheney and Oskoorouchi 1982; Cooper *et al*. 1998; Thusyanthan et al. 2005; Viswanadham and Rajesh 2009; Wang and Zhang 2014). Recently propagation of planar shear band via FEM (Zhang et al. 2019) and a framework for stability analysis of cut slopes in sensitive clays is established based on the criteria for catastrophic shear band propagation (Zhang and Wang 2020).

Progressive failure leads to formation of shear band and it was studied for overconsolidated soil (Burland *et al*. 1977) as well as granular materials (Vardoulakis and Graf; 1985). It is observed that bifurcation and localization occurred before the peak shear resistance. The deformation in shear band depends on the material properties, boundary and geometrical conditions such as the shape and size of the specimen, and material constituents (Sulem and Vardoulakis; 1990). Study reveals that, slip surface forms exactly within the shear zone. Basically shear zone describes the concentration of shear deformation of the slope, which corresponded to the slippage failure of the slip surface. Thus, the failure process mechanism of the slope can be described by Fig. 1.

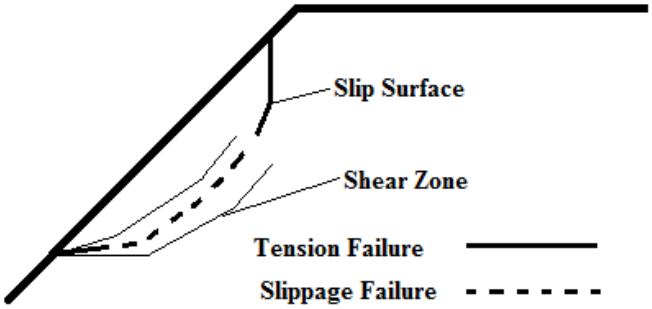

Figure 1 Shear zones and slip surfaces of the slope (Zhang *e. al.*, 2015)

The numerical analysis of progressive failure have been studied using modifications in limit equilibrium methods (Tiande *et al*. 1999; Zhang and Wang 2010; Ahmed et al. 2012; Bai *et al*. 2014). Further strain-softening behavior and strain localization have been analysed using finite element methods (Khoei and Bakhshiani 2005; Arslan and Sture 2008; Conte *et al*., 2010, Sanborn and Prevost 2011; Jiang and Murakami 2012) and finite difference method (Shiau et al. 2011; Esmaeili *et al*., 2013; Hamdhan and Schweiger, 2013; Liu and Zhao, 2013; Isakov and

Moryachkov, 2014). In most of the numerical analysis researchers have used different material models; boundary condition; and geometry of slopes. Potts *et al*., 1990, 1997 have used the elasto-plasticity model for simulating strain-softening during the analysis of the failure surface of a cohesive soil slope. Troncone (2005) used a finite-element program with a nonlocal elasto-viscoplastic model to capture the progressive failure of a slope due to deep excavation. The results of the analysis show that a progressive failure occurred owing to deep excavations carried out at the toe of the slope. Three-dimensional numerical simulations of strain localization also have been performed using Cosserat continuum theory (Khoei *et al*., 2010). Zhang and Yun (2016) have explained the shear deformation localization of progressive failure of soil slopes using "shear element". In the most of studies roller or viscous boundary condition is used. Impact of load on different inclination of slope change over the behavior of slope model has discussed by few researchers (Shinoda *et al*., 2015)

Since shear band formation is an important factor in understanding failures in soil slope. Hence, thorough understanding of the progressive failure mechanism of slopes have been performed. However, previous studies were largely based on the analysis of stress field that cannot be fully captured in field or model tests. As a result, different types of assumptions had to be made to clarify the mechanism of failure process. Also there are still uncertainties regarding when shear bands start to propagate in soil mass.

To analyze the progressive failure strain softening behavior needs to be considered during the numerical analysis. To consider the strain softening behavior Modified Cam-Clay model is one of the option. Very few researchers have considered this aspect of the study. In this paper concept of shear zone was used to describe the formation process of the slip surface (Zhang et al. 2015) of a slope. The impacts of seismic load on soil slope have been studied to investigate the shear band development using Finite Element Method. To simulate the strain localization, softening behavior and development of shear band, a Modified Cam-Clay (MCC) material model was employed. The impact of the inclination of slope is also considered in this study, which is also not considered by other researchers in their studies.

Statement of Problems

In order to study the impact of seismic load on shear band development in soil slope, three different inclination of model size 115 m long, 50 m wide and 60 m tall has been considered

(Fig. 2). Three models of different inclinations (Vertical: Horizontal) 1:1.75, 1:2 and 1:2.25 are set up. Vertical height of slope is assumed constant. Displacement and acceleration response at Toe of Slope (Node A), Mid of Slope (Node B) and at Crest of Slope (Node C) are considered.

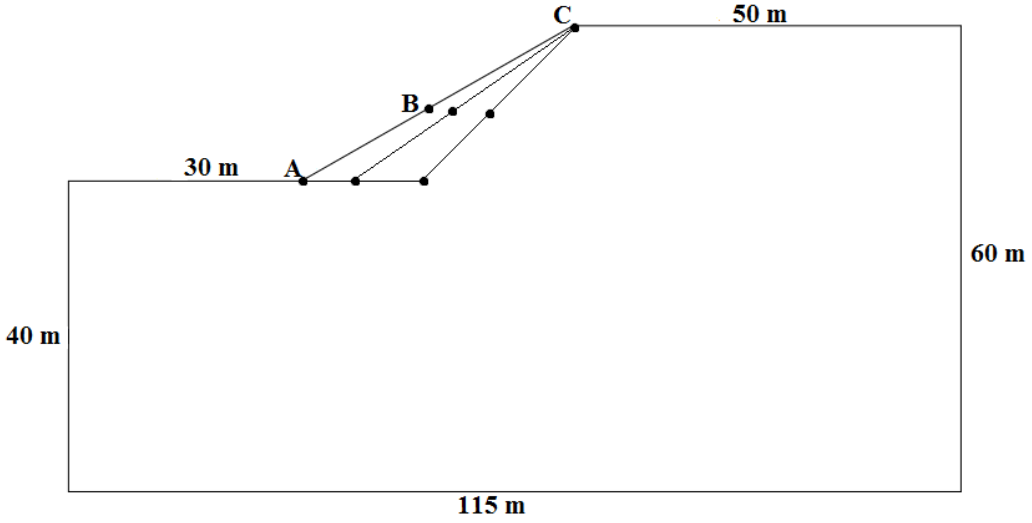

Figure 2 Slope model

Input motion of Chamoli earthquake (1999) with peak ground acceleration (PGA) of 0.36g has applied on the base of Soil Slope to investigate the shear band development (Fig. 3).

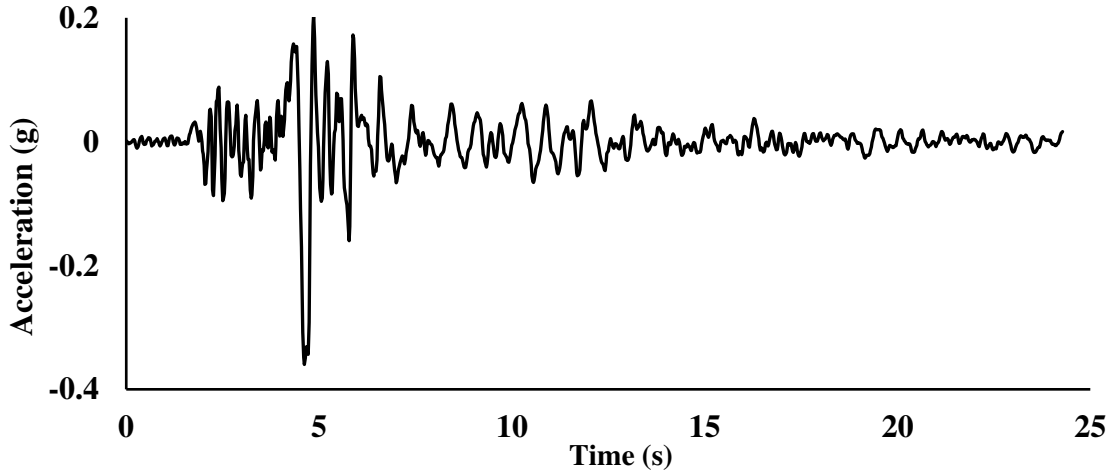

Figure 3 Chamoli (1999) earthquake acceleration-time history

Modeling of Soil Slope

A finite element model with 15 node triangular element in plain strain condition were used to find the localized shear strain in the slope and development of shear band (Fig. 4). Lysmer and

Kuhlemeyer (1969) boundary was applied at the side boundaries of model. Modified Cam-Clay (MCC) material model for soil was employed to observe the softening behavior in soil slope.

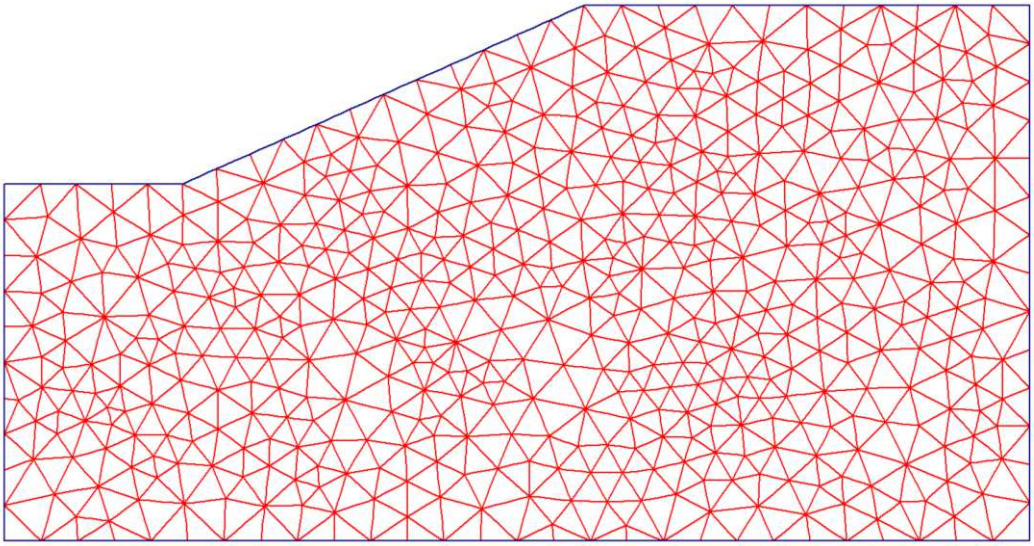

Figure 4 FEM model of slope

The material parameters which are essential to define MCC material model is shown in Table 1 and geometrical properties of soil slope is shown in Table 2.

Table 1. Material Behavior of Soil Slope

Parameters of MCC Material Model	
Poisson's ratio (ν)	0.3
Swelling Index (κ)	0.05
Compression Index (λ)	0.08
Tangent on Critical State Line (M)	0.701
Initial Void Ratio (e)	0.37

Table 2. Soil Slope Parameters

Properties of soil	
Dry density of Soil	19.6 kN/m^3
Damping in soil	15%
Rayleigh damping Co-efficient α and β	0.2805 & 0.1212
Slope Inclination	1:1.75, 1:2 and 1:2.25

Strain analysis was employed to investigate the deformation behavior of the slope using PLAXIS 2D. The maximum shear strain was selected to describe the shear deformation of the slope. The eight node quadrilateral elements were used to find the maximum shear strain in the soil slope.

The acceleration and displacement response at above discussed response points with three different inclinations are calculated. Before proceeding the analysis a brief introduction of MCC material model is discussed in below section.

Yield Function of Modified Cam-Clay (MCC) Model

Elasto-Plastic strain hardening/softening model can be analysed using critical state theory. Cam-Clay (CC) and Modified Cam-Clay (MCC) models are based on the critical state theory. The basic assumption that there is a logarithmic relationship between the mean stress and the void ratio. Three important behavior of soil viz. strength, compression or dilatancy (the volume change that occurs with shearing), and Critical State at which soil elements can experience unlimited distortion without any changes in stress or volume are suitably analysed with CC and MCC models.

The difference between the CC and the MCC is that the yield surface of the MCC is described by an ellipse and therefore the plastic strain increment vector (which is perpendicular to the yield surface) for the largest value of the mean effective stress is horizontal, and hence no incremental deviatoric plastic strain takes place for a change in mean effective stress (for purely hydrostatic states of stress). In critical state mechanics, the state of a soil sample is characterized by three parameters, mean stress, deviatoric stress, and specific volume. The specific volume υ is defined as

$$\upsilon = 1 + e \tag{1}$$

Where, e is the void ratio.

The models assume that when a soft soil sample is slowly compressed under isotropic stress conditions, and under perfectly drained conditions, the relationship between specific volume and mean stress consists of a straight virgin consolidation line or normal compression line and a set of straight swelling lines i.e. unloading-loading lines (Fig. 4).

The virgin consolidation line in Figure 5 is defined by the equation

$$\upsilon = N - \lambda \ ln \ (-p) \tag{2}$$

While the equation for a swelling line has the form

$$\upsilon = \upsilon_s - \kappa \ ln \ (-p) \tag{3}$$

The values λ, κ and N are characteristic properties of a particular soil.

λ = slope of the normal compression (virgin consolidation) line on $\upsilon - ln\ p$ plane.

κ = slope of swelling line.

N = specific volume of normal compression line at unit pressure, and is dependent on the units of measurement.

υ_s differs for each swelling line, and depends on the loading history of a soil.

If the current state of a soil is on the virgin consolidation line the soil is described as being normally consolidated. If the stress state is below the line, it becomes overconsolidated. In general, soil does not exist outside the virgin consolidation line; when it does that state is unstable.

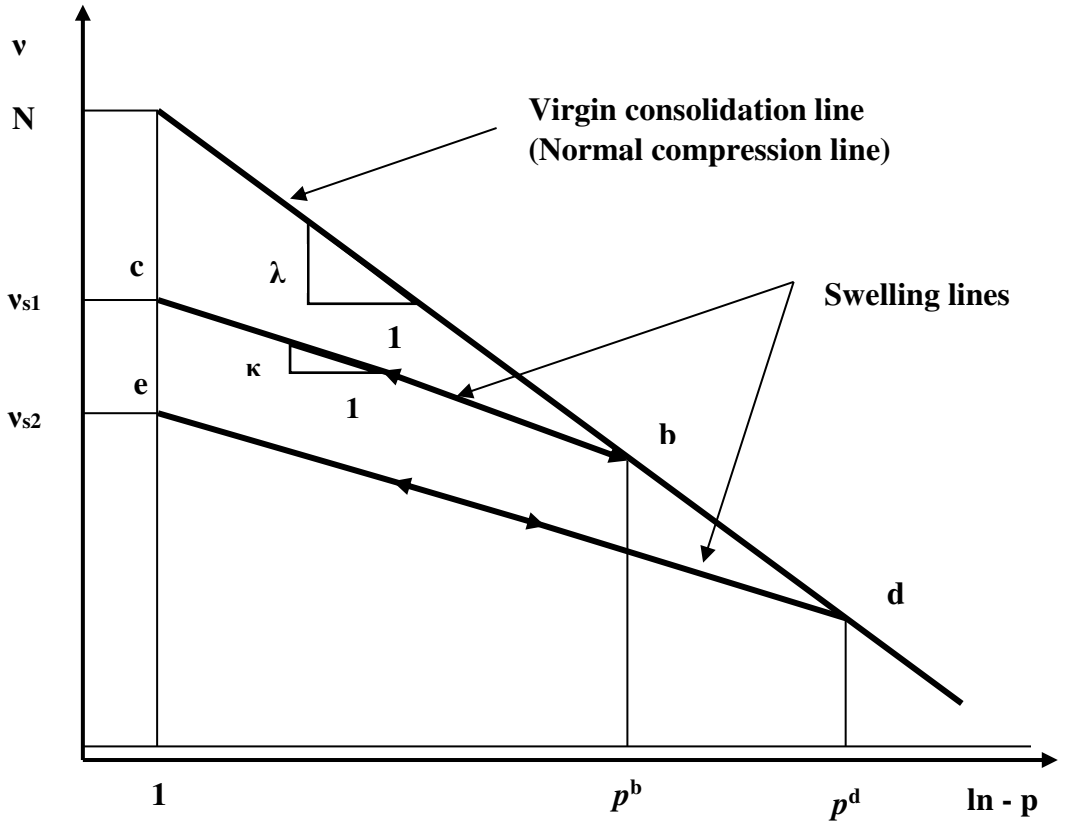

Figure 5 Typical behavior of clays in consolidation (Oedometer) test

In the Modified Cam-Clay model, a logarithmic relation is assumed between void ratio e and the mean effective stress 'p' in virgin isotropic compression, which can be formulated as:

$$e - e^0 = -\lambda \ln (p/p^0) \tag{4}$$

In which, λ is the Cam-Clay isotropic compression index.

It determines the compressibility of the material in primary loading. During unloading and reloading, a different line is followed, which can be formulated as:

$$e - e^0 = - \kappa \ln (p/p^0) \quad (5)$$

The parameter κ is the Cam-Clay isotropic swelling index, which determines the compressibility of material in unloading and reloading. In fact, an infinite number of unloading and reloading lines exists in p' – e - plane each corresponding to a particular value of the preconsolidation stress p_p. The yield function of the Modified Cam-Clay model is defined as:

$$f = \frac{q^2}{M^2} + p'(p' - p_p) \quad (6)$$

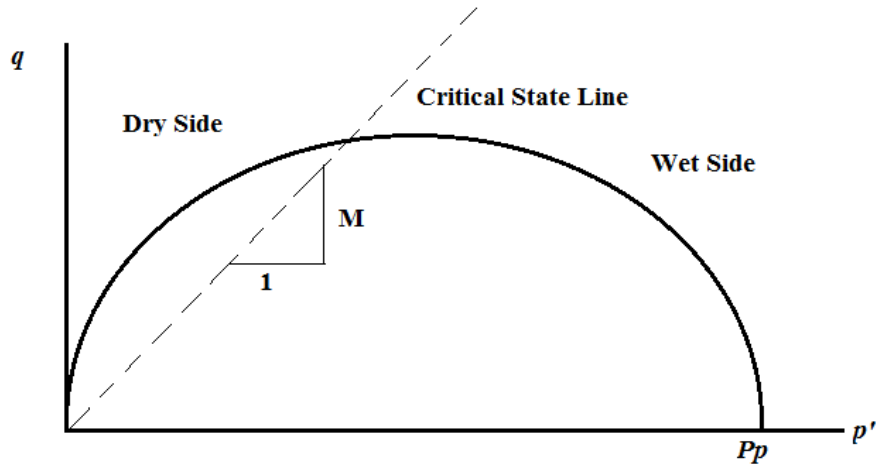

Figure 6 Yield surface of the mcc model in p' – q - plane

The yield surface (f = 0) represents an ellipse in p' – q - plane as indicated in Fig. 6. The yield surface is the boundary of the elastic stress states. Stress paths within this boundary only give elastic strain increments, whereas stress paths that tend to cross the boundary generally give both elastic and plastic strain increment

In p'- q - plane, the top of the ellipse intersects a line that we can be written as:

$$q = mp' \quad (7)$$

This line is called the critical state line (CSL) and gives the relation between p' and q in a state of failure (i.e. the critical state). The constant M is the tangent of the critical state line and determines the extent to which the ultimate deviatoric stress, q depends on the mean effective stress, p. Hence, M can be regarded as a friction constant. Moreover, M determines the shape of the yield surface (height of the ellipse).

In fact an infinite number of ellipses exist, each corresponding to a particular value of p_p . The left hand side of the yield ellipse (often described as the 'dry side' of the critical state line) may

be thought of as a failure surface. In this region plastic yielding is associated with softening, and therefore failure. The values of q can become unrealistically large in this region.

Sustained shearing of a soil sample eventually leads to a state in which further shearing can occur without any changes in stress or volume. This means that at this condition, known as the critical state, the soil distorts at constant state of stress with no volume change. This state is called the Critical State and characterized by the Critical State Line (CSL). In pq′− plane the CSL is a straight line passing through the origin with the slope equal to M, one of the characteristic of the material that is the main parameter in the definition of yield surface.

The current state of a soil can be described by its stress state (p, q,), specific volume υ, and yield stress, pc (also known as preconsolidation pressure is a measure of the highest stress level the soil has ever experienced). The ratio of preconsolidation pressure to current pressure is known as the over-consolidation ratio (OCR).

Hardening and Softening Behavior

Plastic volumetric strain and compaction of material causing hardening of material which in results in reduction in void ratio and specific volume. Considering an increment of load from step *n* to *n + 1* the expansion of the yield surface is defined by the increase in preconsolidation pressure.

$$p_{c_{n+1}} = p_{c_{n+1}} \exp\left(\frac{v_n \Delta \varepsilon_v^p}{\lambda - \kappa}\right) \tag{8}$$

If yielding occurs to the right of the point at which the CSL intersects a yield surface, hardening behavior, accompanied by compression, is exhibited. This side of the yield surface is known as the wet or subcritical side.

If yielding occurs to the left of the intersection of the CSL and yield surface (called the dry or supercritical side), the soil material exhibits softening behavior, which is accompanied by dilatancy (increase in volume). In softening regimen the yield stress curve decreases after the stress state touches the initial envelope.

Results and Discussion

The behavior and development of shear band are analyzed for three different inclinations. To understand the development of the shear band results at four different steps i.e. immediate act of seismic load up to 1.5 sec, 1.5 sec to 2.5 sec, 2.5 sec to 5.9 sec and after the completion duration of earthquake considered. Displacement and acceleration response of soil slope for these inclinations are also presented here.

Behavior and Development of Shear Band in Soil Slopes

Fig. 7 shows the behavior of soil slope and development of shear band for inclination of 1:1.75. The deformation pattern between start of seismic load to end of seismic load in four steps are depicted here. Fig. 7(a) corresponds to immediate application of seismic load to 1.5 sec and it can be observe that the failure in slope is tension failure. Due to the tension, formation of slip surface near the crest of the slope takes place.

Fig. 7(b) shows the strain localization initiate at toe of the slope after 1.5 sec in the slope mass. In case of strain softening behavior of soil, progressive failure starts to occur at toe of the slope and progress towards crest of slope. This result is compared and validated with Zhang *et al.* (2007).

Fig. 7(c) shows the formation of shear band up to half of the height of slope and progressing towards the crest of slope. This is another significance of progressive failure in strain softening behavior. This formation of shear band is occurring at peak amplitude of seismic load. The deep yield zone is likely to observe near the crest of slope. The significance of deep yield zone is formation of tension failure at that zone. This was observe at the initiation of seismic load i.e. in first step.

Fig. 7(d) shows the accumulation of strain is completely within the shear band. Complete mobilization of plastic strain in slope mass and formation of shear band along slope has also taken place. It can also be observed that the formation of shear band start from the toe to crest of slope. So we can say that the mobilization of plastic strain in softening material is a progressive phenomenon and it happens because of inertial effects.

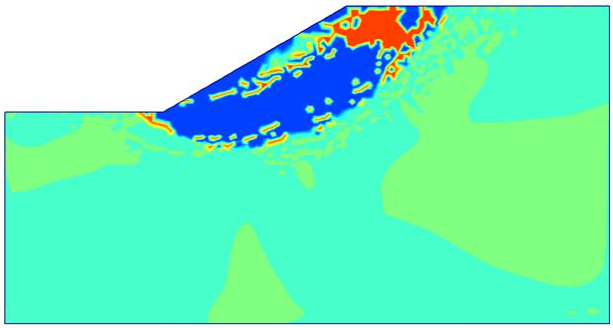

(a) Immediate application of seismic load upto 1.5 sec. duration

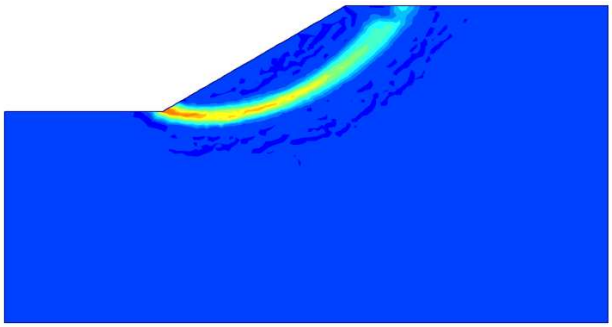

(b) 1.5 sec. to 2.5 sec. duration

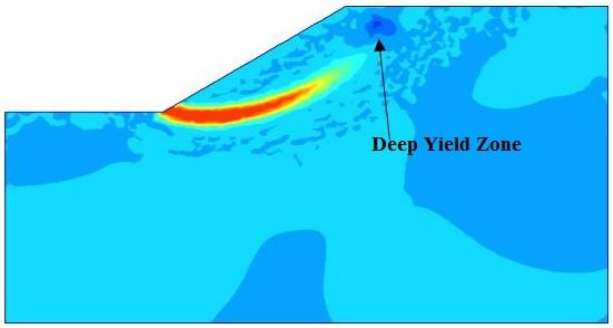

(c) 2.5 sec. to 5.9 sec.

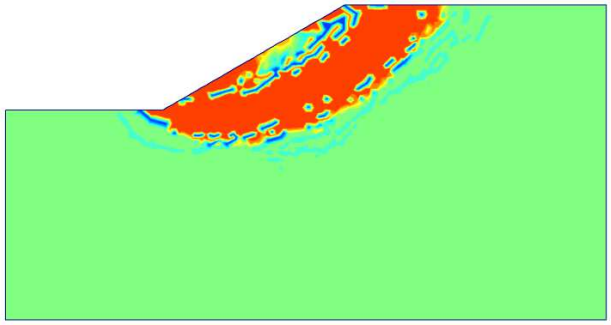

(d) After completion of seismic load

Figure 7 Behavior of the soil slope and development of shear band at various duration of times for 1:1.75 inclination

Zhang *et al.* (2007) analysed the slope in FLAC3D using Non-Linear Mohr-Coulomb material model. At the very first step it was found that the progressive failure in softening type soil starts from the toe as shown in Fig. 8(a). The current study is illustrated in Fig. 8(b). It can be observed that the progressive failure in slope start from toe and progress towards crest of slope. It is validating the present model. From Figure 7 & 8 the strain localized within the slope mass and starts increasing from toe to crest of the slope.

(a) At start of seismic load FLAC3D model (Zhang et al., 2007)

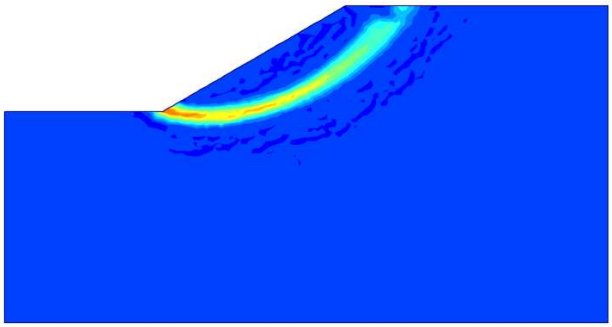

(b) Initiation of Strain Localization and Shear Band (Current study)

Figure 8 Validation of strain localization in progressive failure

Fig. 9 and Fig.10 shows the behavior of soil slope and development of shear band for inclination of 1:2 and 1:2.25 respectively. It can be observed in both of the cases that the overall slope remain stable and strain localization takes place at toe (Fig. 9b, c and Fig 10 b,c). Fig. 9 d shows the formation of shear band near to the toe, but further propagation of the shear band was not taken place. Since the stress mobilized in this condition (Fig. 9 and 10) is lesser than the resisting stress, so deviation in the behavior of the slope is taking place.

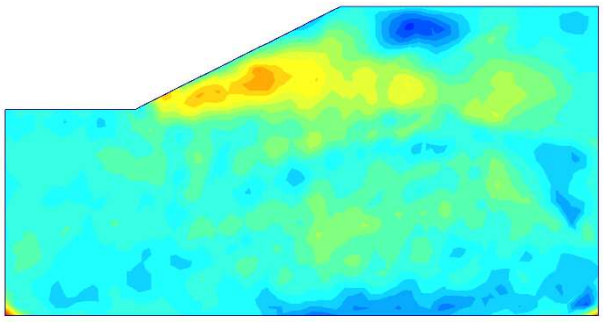

(a) Immediate application of seismic load upto 1.5 sec. duration

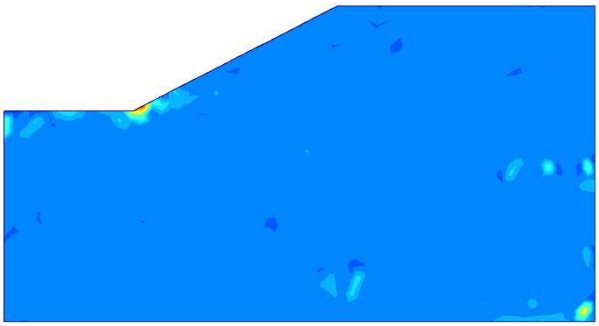

(b) 1.5 sec. to 2.5 sec. duration

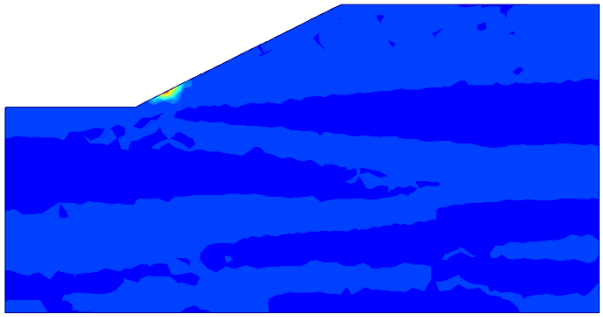

(c) 2.5 sec. to 5.9 sec.

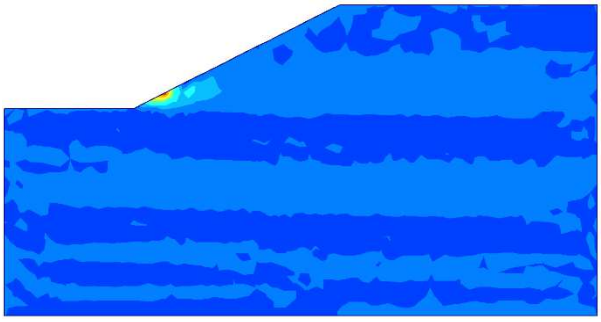

(d) After completion of seismic load

Figure 9 Behavior of the soil slope and development of shear band at various duration of times for 1:2 inclination

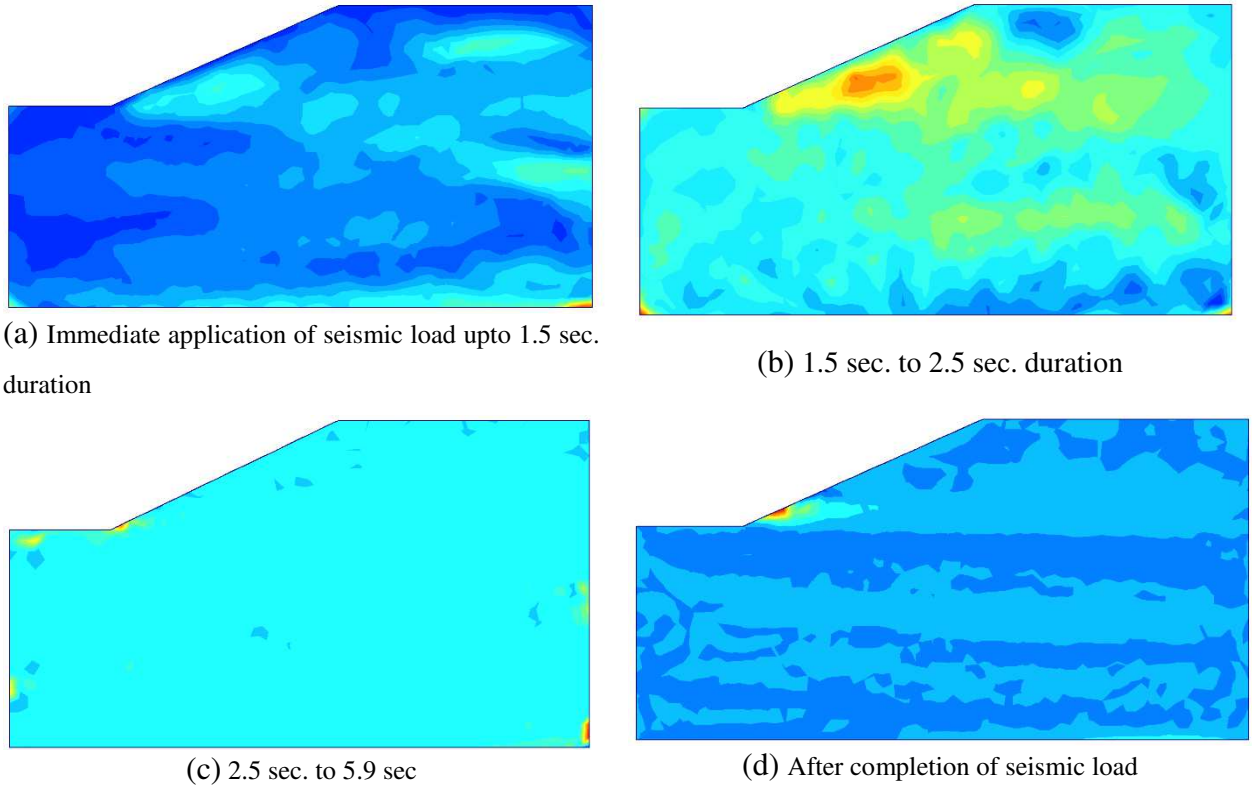

(a) Immediate application of seismic load upto 1.5 sec. duration

(b) 1.5 sec. to 2.5 sec. duration

(c) 2.5 sec. to 5.9 sec

(d) After completion of seismic load

Figure 10 Behavior of the soil slope and development of shear band at various duration of times for 1:2.25 inclination

Effect of Inclination on soil slope response under seismic condition

Response of slope for three different inclinations at three points Toe of Slope A, Mid of Slope B and Crest of Slope C have been observed. To describe the impact of seismic load at these points, peak ground acceleration amplification factor (Ω) and maximum displacement response is used. Peak ground acceleration amplification factor is the ratio between the peak acceleration (PGA_o) at each point on the slope surface and the peak acceleration (PGA_i) of seismic wave input from the bottom of model.

$$\Omega = \frac{PGA_o}{PGA_i} \quad (1)$$

PGA Amplification factor for slope 1:1.75, 1:2 and 1:2.25 have been obtained at above mentioned points. Response of slope at points A, B and C are plotted in Fig. 11. It can be observed that the peak ground acceleration amplification factor increases with increase in the slope (Fig. 11). This factor is also found minimum at the toe, while maximum at crest. Similar

response is found for all slopes. But the coefficient is greater at crest (point C) for higher slope i.e. for slope 1:1.75.

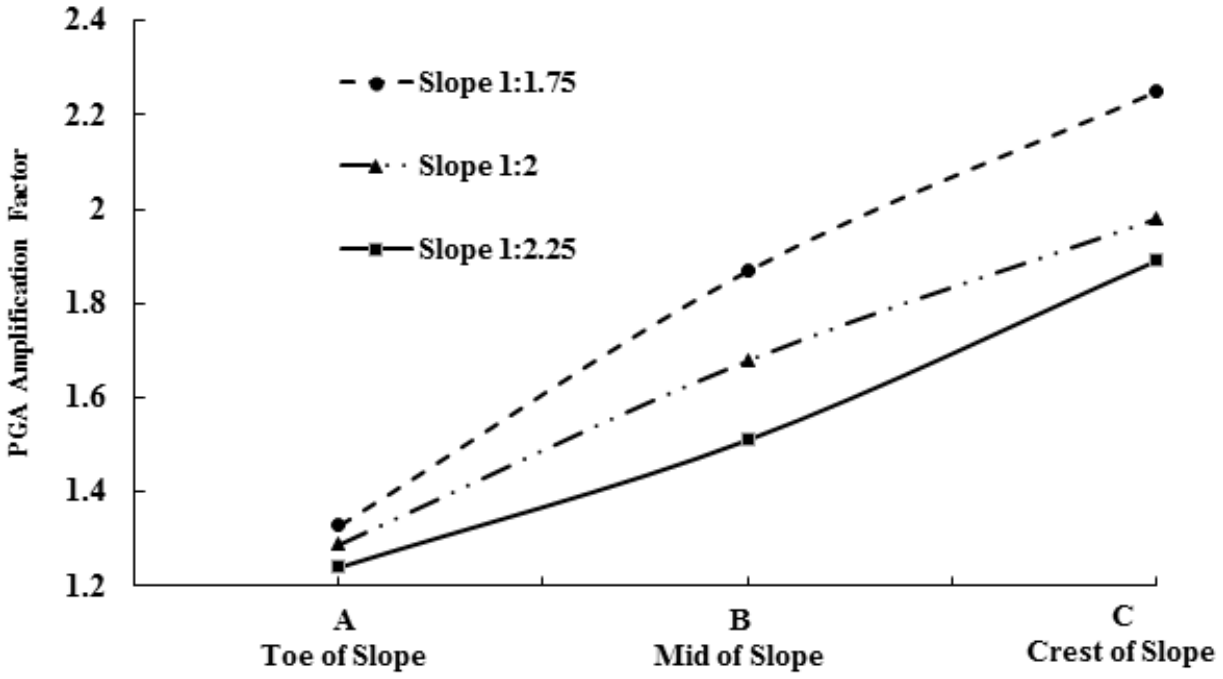

Figure 11Horizontal PGA Amplification factor for slope

The maximum displacement response of slope is presented in Fig. 12. It can be observed that the displacement at point C i.e. the point at crest is higher for all slopes. With increase in the height of the point from the toe, displacement of the point is found increasing. It means under seismic load relative displacement exist between two different points of the slope. It can be further observed that with increase in the inclination of the slope displacement of the points on the surface of the slope (Point A, B, and C) increases. Here it can also be observed that at higher inclination of slope curve showing the displacement of point is not linear like at lower inclination. In case of higher inclination, displacement of point increases with increase in the height of the point from toe, but rate of increment of displacement decreases. In other words it can be said that tendency of relative displacement decreases at higher inclination of the slope.

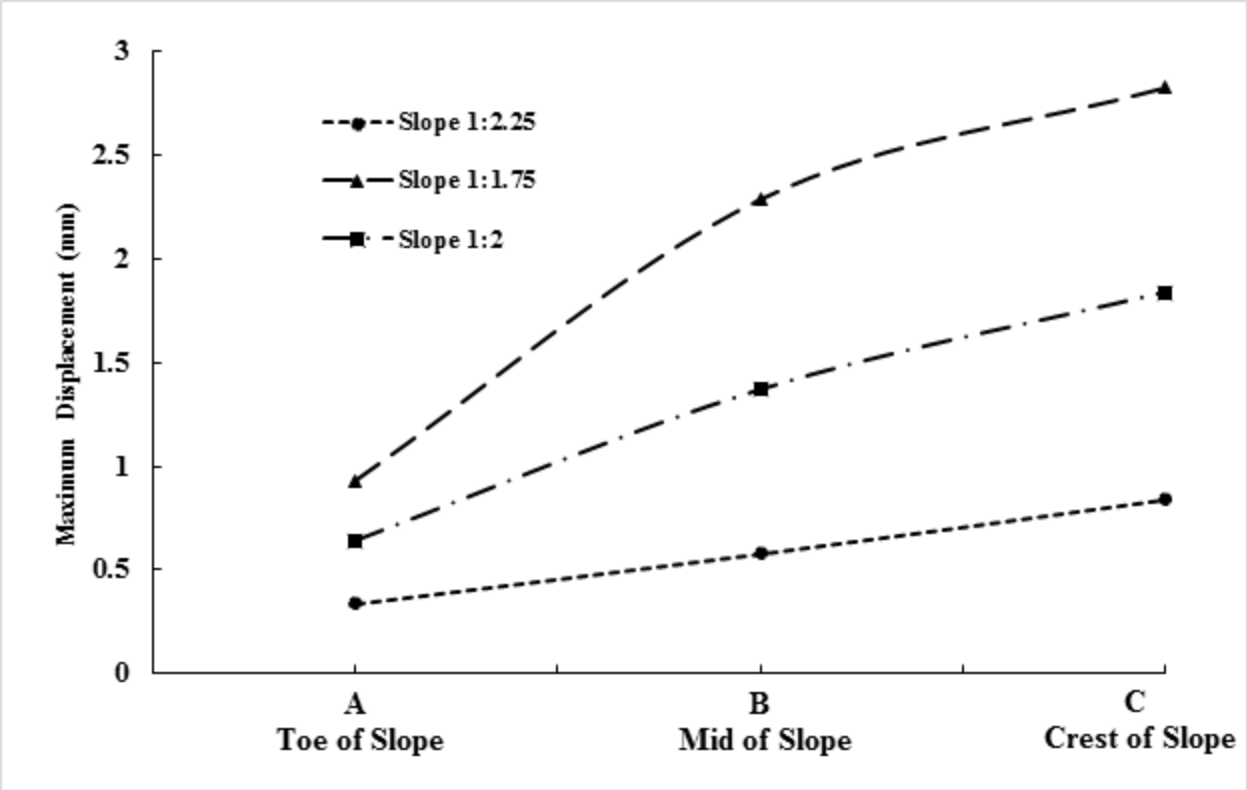

Figure 12 Horizontal Displacements for Slope

Summary and Conclusions

1. The continuous yield zone along the failure surface was not formed. It was observed that deep yield zone for slope inclination 1:1.75 and 1:2.25. Which causes the tension failure in the slope.
2. It is also concluded that none of the slopes are stable under seismic action, but the instability of different slopes with inclination varies. The slope with an inclination of 1:2.25 is relatively stable. The slope with an inclination of 1:2 has local failure, but not destroyed as a whole.
3. The slope with an inclination of 1:1.75 has a complete formation of shear band along the slip surface. The slope is destroyed as a whole.
4. Development of shear band occurred along the slope with application of seismic load but delay of complete development of shear band in slope due to inertial effects.
5. Peak ground acceleration amplification factor increases with increase in the slope.
6. In case of higher inclination, displacement of point increases with increase in the height of the point from toe, but rate of increment of displacement decreases.

Author contribution

VK: Conceptualization, methodology, analysis and writing-original draft. SK: Supervision, review and editing, final correction, helping in preparation of draft.

Refrences

1. Torabi, A., Braathen, A., Cuisiat, F., and Fossen, H. 2007. "Shear zones in porous sand: Insights from ring-shear experiments and naturally deformed sandstones." *Tectonophysics*, 437, 37–50.)
2. Skempton, A.W., 1964. Long-term stability of clay slopes. *Géotechnique*, 14(2):77-101.
3. Vardoulakis, I. _1996_. "Deformation of water-saturated sand: I. Uniform undrained deformation and shear banding." *Geotechnique*, 46_3_, 441–456.
4. Conte, E., Silvestri, F., Troncone, A., 2010. Stability analysis of slopes in soils with strain-softening behaviour. *Computers and Geotechnics*, **37**(5):710-722.
5. Sadrekarimi, A. _2009_. "Development of a new ring shear apparatus for investigating the critical state of sands." Ph.D. thesis, Univ. of Illinois at Urbana-Champaign, Urbana, Ill.)
6. Mesri, G., Shahien, M., 2003. Residual shear strength mobilized in first-time slope failures. Journal of Geotechnical and Geoenvironmental Engineering.
7. Locat, A., Leroueil, S., Bernander, S., Demers, D., Jostad, H.P., Ouehb, L., 2011. Progressive failures in eastern Canadian and Scandinavian sensitive clays. Canadian Geotechnical Journal, 48(11):1696-1712.
8. (Vallejo, L. E. _1987_. "The influence of fissures in a stiff clay subjected to direct shear." *Geotechnique*, 37_1_, 69–82.
9. Saada, A. S., Bianchini, G. F., and Liang, L. _1994_. "Cracks, bifurcation and shear bands propagation in saturated clays." *Geotechnique*, 44_1_, 35–64
10. Alshibli, K. A., and Akbas, I. S. _2007_. "Strain localization in clay: Plane strain versus triaxial loading conditions." *Geotech. Geologic. Eng.*, 25, 45–55)
11. Harris, W. W. _1994_. "Localization of loose granular soils and its effect on undrained steady state strength." Ph.D. thesis, Northwestern Univ.
12. Peters, J., Lade, P., and Bro, A. _1988_. "Shear band formation in triaxial and plane strain tests." *Advanced triaxial testing of soil and rock, ASTM, STP977*, R. Donaghe, R. Chaney, and M. Silver, eds., ASTM, West Conshohocken, Pa., 604–627.
13. Rice, J. _1976_. "The localization of plastic deformation." *Proc., 14th Int. Congress on Theoretical and Applied Mechanics*, Vol. 1, North Holland Publishing, Delft, The Netherlands, 207.
14. Vardoulakis, I., and Graf, B. _1985_. "Calibration of constitutive models for granular materials using data from biaxial experiments." *Geotechnique*, 35_3_, 299–317.
15. J. Sulem and I.G. Vardoulakis, Bifurcation analysis of the triaxial test on rock specimens. A theoretical model for shape and size effect, Acta Mechanica, 32, pp. 195–212, (1990)].

16. Burland, J. B., Longworth, T. I., and Moore, J. F. A. (1977). “A study of ground movement and progressive failure caused by a deep excavation in Oxford clay.” Geotechnique, 27(4), 557–591.
17. Wang, L. P., and Zhang, G. (2014). “Progressive failure behavior of pile reinforced clay slopes under surface load conditions.” Environ. Earth Sci., 71(12), 5007–5016.
18. Zhang, G., Hu, Y., and Wang, L. P. (2015). “Behaviour and mechanism of failure process of soil slopes.” Environ. Earth. Sci., 73(4), 1701–1713
19. Cheney, J. A., and Oskoorouchi, A. M. (1982). “Physical modeling of clay slopes in the drum centrifuge.” Transportation Research Record, 872, 1–7
20. Cooper, M. R., Bromhead, E. N., Petley, D. J., and Grants, D. I. (1998). “The Selborne cutting stability experiment.” G_eotechnique, 48(1), 83–101.
21. Thusyanthan, N. I., Madabhushi, S. P. G., and Singh, S. (2005). Seismic performance of geomembrane placed on a slope in a MSW landfill cell–A centrifuge study, Geotechnical Special Publication, 130–142, ASCE, Reston, VA, 2841–2852.
22. Viswanadham, B. V. S., and Rajesh, S. (2009). “Centrifuge model tests on clay based engineered barriers subjected to differential settlements.” Appl. Clay Sci., 42(3–4), 460–472.
23. Zhang, G., Hu, Y., and Wang, L. P. (2015). “Behaviour and mechanism of failure process of soil slopes.” Environ. Earth. Sci., 73(4), 1701–1713
24. Tiande, M., Chongwu, M., and Shengzhi, W. (1999). “Evolution model of progressive failure of landslides.” J. Geotech. Geoenviron. Eng., 10 .1061/(ASCE)1090-0241(1999)125:10(827), 827–831.
25. Zhang, G., and Wang, L. P. (2010). “Stability analysis of strain-softening slope reinforced with stabilizing piles.” J. Geotech. Geoenviron. Eng., 10.1061/(ASCE)GT.1943-5606.0000368, 1578–1582.
26. Ahmed, A., Ugai, K., and Yang, Q. (2012). “Assessment of 3D slope stability analysis methods based on 3D simplified Janbu and Hovland methods.” Int. J. Geomech., 10.1061/(ASCE)GM.1943 -5622.0000117, 81–89.
27. Bai, T., Qiu, T., Huang, X., and Li, C. (2014). “Locating global critical slip surface using the Morgenstern-Price method and optimization technique.” Int. J. Geomech., 10.1061/(ASCE)GM.1943-5622.0000312, 319–325.
28. Shiau, J., Merifield, R., Lyamin, A., and Sloan, S. (2011). “Undrained stability of footings on slopes.” Int. J. Geomech., 10.1061/(ASCE)GM .1943-5622.0000092, 381–390.
29. Esmaeili, M., Nik, M., and Khayyer, F. (2013). “Experimental and numerical study of micropiles to reinforce high railway embankments.” Int. J. Geomech., 10.1061/(ASCE)GM.1943-5622.0000280, 729–744.
30. Hamdhan, I. N., and Schweiger, H. F. (2013). “Finite elementmethod-based analysis of an unsaturated soil slope subjected to rainfall infiltration.” Int. J. Geomech., 10.1061/(ASCE)GM.1943-5622.0000239, 653–658.

31. Liu, F., and Zhao, J. (2013). “Limit analysis of slope stability by rigid finiteelement method and linear programming considering rotational failure.” Int. J. Geomech., 10.1061/(ASCE)GM.1943-5622.0000283, 827–839.
32. Isakov, A., and Moryachkov, Y. (2014). “Estimation of slope stability using two-parameter criterion of stability.” Int. J. Geomech., 10.1061 /(ASCE)GM.1943-5622.0000326, 06014004.
33. Potts, D. M., Dounias, G. T., and Vaughan, P. R. (1990). “Finite element analysis of progressive failure of Carsington embankment.” Geotechnique, 40(1), 79–101
34. Potts, D. M., Kovacevic, N., and Vaughan, P. R. (1997). “Delayed collapse of cut slopes in stiff clay.” Geotechnique, 47(5), 953–982
35. Khoei, A. R., and Bakhshiani, A. (2005). “A hypoelasto-viscoplastic endochronic model for numerical simulation of shear band localization.” Finite Elem. Anal. Des., 41(14), 1384–1400.
36. Arslan, H., and Sture, S. (2008). “Finite element simulation of localization in granular materials by micropolar continuum approach.” Comput. Geotech., 35(4), 548–562.
37. Conte, E., Silvestri, F., and Troncone, A. (2010). “Stability analysis of slopes in soils with strain-softening behaviour.” Comput. Geotech., 37(5), 710–722.
38. Sanborn, S. E., and Prevost, J. H. (2011). “Frictional slip plane growth by localization detection and the extended finite element method (XFEM).” Int. J. Numer. Anal. Methods Geomech., 35(11), 1278–1298.
39. Jiang, M. J., and Murakami, A. (2012). “Distinct element method analyses of idealized bonded-granulate cut slope.” Granular Matter, 14(3), 393–410
40. Troncone, A. (2005). “Numerical analysis of a landslide in soils with strainsoftening behavior.” G_eotechnique, 55(8), 585–596.
41. Khoei, A. R., Yadegari, S., and Biabanaki, S. O. R. (2010). “3D finite element modeling of shear band localization via the micro-polar Cosserat continuum theory.” Comput. Mater. Sci., 49(4), 720–733.
42. Zhang, Ga and Hu Yun (2016). “Numerical Modeling of Failure Process of Soil Slopes.” ASCE, International Journal of Geomechanics, 06016031 (1-8)
43. Triantafyllidist, N., Needleman A., Tvergaard, V. (1982).” On the development of shear band in pure bending”. International Journal of Solids and Structures 18(2):121-138
44. Needleman, A., 1989. “Dynamic Shear Band Development in Plane Strain”. Journal of applied mechanics, vol. 56/1-9.
45. Shinoda, M.’ Watanabe, K., Sanagawa, T., Abe, K., Hidetaka, N., Tadashi, K., Susumu, N. (2015); “Dynamic behavior of slope models with various slope inclinations”. Soils and Foundations Volume 55, Issue 1, February 2015, Pages 127-142.
46. Zhang, W., Randolph, M.F., Puzrin, A.M. *et al.* Criteria for planar shear band propagation in submarine landslides along weak layers. *Landslides* **17,** 855–876 (2020). https://doi.org/10.1007/s10346-019-01310-8

47. Zhang, W. and Wang, D. (2020); Stability analysis of cut slope with shear band propagation along a weak layer. Computers and Geotechnics 125(1):103676 DOI: 10.1016/j.compgeo.2020.103676